JB
Journals.ASM.org

The Ctp Type IVb Pilus Locus of *Agrobacterium tumefaciens* Directs Formation of the Common Pili and Contributes to Reversible Surface Attachment

Yi Wang, Charles H. Haitjema,* Clay Fuqua

Department of Biology, Indiana University, Bloomington, Indiana, USA

***Agrobacterium tumefaciens* can adhere to plant tissues and abiotic surfaces and forms biofilms. Cell surface appendages called pili play an important role in adhesion and biofilm formation in diverse bacterial systems. The *A. tumefaciens* C58 genome sequence revealed the presence of the *ctpABCDEFGHI* genes (cluster of type IV pili; Atu0216 to Atu0224), homologous to *tad*-type pilus systems from several bacteria, including *Aggregatibacter actinomycetemcomitans* and *Caulobacter crescentus*. These systems fall into the type IVb pilus group, which can function in bacterial adhesion. Transmission electron microscopy of *A. tumefaciens* revealed the presence of filaments, significantly thinner than flagella and often bundled, associated with cell surfaces and shed into the external milieu. In-frame deletion mutations of all of the *ctp* genes, with the exception of *ctpF*, resulted in nonpiliated derivatives. Mutations in *ctpA* (a pilin homologue), *ctpB*, and *ctpG* decreased early attachment and biofilm formation. The adherence of the *ctpA* mutant could be restored by ectopic expression of the paralogous *pilA* gene. The Δ*ctpA* Δ*pilA* double pilin mutant displayed a diminished biovolume and lower biofilm height than the wild type under flowing conditions. Surprisingly, however, the *ctpCD*, *ctpE*, *ctpF*, *ctpH*, and *ctpI* mutants formed normal biofilms and showed enhanced reversible attachment. In-frame deletion of the *ctpA* pilin gene in the *ctpCD*, *ctpE*, *ctpF*, *ctpH*, and *ctpI* mutants caused the same attachment-deficient phenotype as the *ctpA* single mutant. Collectively, these findings indicate that the *ctp* locus is involved in pilus assembly and that nonpiliated mutants, which retain the CtpA pilin, are proficient in attachment and adherence.**

Agrobacterium tumefaciens is a plant pathogen in the family *Rhizobiaceae* related to nitrogen-fixing symbionts of leguminous plants. Unlike the rhizobia, *A. tumefaciens* causes crown gall disease, which is characterized by the formation of neoplastic tumors at sites of bacterial infection, in a wide variety of plants (1). It is well known that *A. tumefaciens* can genetically transform plants by transferring a segment of its own DNA (T-DNA) into the genomes of plants (1). *A. tumefaciens* is widely used to engineer transgenic plants in agricultural biotechnology (2).

Cell attachment to tissues and biofilm formation by *A. tumefaciens* contribute to plant infection and environmental persistence of the pathogen. *A. tumefaciens* is able to form complex, structured biofilms on both plant roots and abiotic surfaces (3–5). The mechanisms of attachment and biofilm formation in *A. tumefaciens* are an area of active study. Initially, flagellar motility enables *A. tumefaciens* to contact target surfaces, including chemotaxis toward attractants produced by wounded plant tissues (6, 7). Cells transiently attach to the surface, and then a more stable association is formed. Early stages of *A. tumefaciens* biofilms on abiotic surfaces are visible in laboratory cultures in defined growth medium with a glucose or mannitol carbon source after a day of incubation (4). These biofilms are relatively shallow layers of cells, of which a large proportion are attached via a single pole (3, 4). Over several days of incubation, the biofilm structure matures with the formation of multicellular microcolonies (4, 8).

Several adherence factors have been reported to function in attachment and biofilm formation (7, 9–11). Flagellar motility is required for efficient biofilm formation in static culture (7). *A. tumefaciens* C58 produces multiple exopolysaccharides (EPSs), including the unipolar polysaccharide (UPP), cellulose, and β-1,2-glucans, which can contribute to biofilm formation (9, 10, 12, 13). A calcium-dependent outer membrane protein called rhicadhesin is reported to promote the attachment of bacteria to plant cell walls, but the gene that encodes this activity has never been identified (11).

Pili are filamentous, proteinaceous, extracellular appendages on bacterial surfaces (also known as fimbriae). These structures can function in horizontal gene transfer, motility, and, in many cases, adhesion (14, 15). Several types of pili exist in *A. tumefaciens* C58. Three forms of conjugal pili are independently involved in conjugal transfer activities of the two endogenous plasmids. The *avhB* genes located on the pAtC58 plasmid (16) and the *trb* genes on the Ti plasmid (17) contribute to interbacterial plasmid conjugal transfer. Also encoded by several of the virulence genes in the *virB* operon located on the Ti plasmid are the T pili, which are involved in the association with plants that leads to T-DNA transfer and genetic transformation. Ti plasmid conjugal transfer and virulence gene expression are tightly regulated on the Ti plasmid (18, 19), and these pili are not produced in standard laboratory culture. In contrast to the Ti plasmid, the pAtC58 plasmid is active for conjugal transfer in culture, and the presumptive pAtC58 conju-

Received 16 March 2014 Accepted 4 June 2014
Published ahead of print 9 June 2014
Address correspondence to Clay Fuqua, cfuqua@indiana.edu.
* Present address: Charles H. Haitjema, Department of Chemical Engineering, University of California, Santa Barbara, Santa Barbara, California, USA.
Supplemental material for this article may be found at http://dx.doi.org/10.1128/JB.01670-14.

doi:10.1128/JB.01670-14

gal pili could be produced in culture but have never been defined (16).

In addition to these plasmid-encoded conjugal pili in *A. tumefaciens*, there have also been electron microscopic studies that revealed the presence of what were described as common pili (20). The complete genome sequence of *A. tumefaciens* C58 (21, 22) revealed a chromosomally located nine-gene cluster on the circular chromosome that was annotated as the *ctp* (cluster of type IV pili) locus (*ctpABCDEFGHI*), homologous to genes that encode a subset of type IV pili best characterized as the Cpa pilus cluster of *Caulobacter crescentus* and the *tad* (tight adherence) locus in *Aggregatibacter actinomycetemcomitans* (23, 24). *tad*-type loci exist in widespread bacteria, including *Yersinia pestis*, *Vibrio cholerae*, *Mycobacterium tuberculosis*, *Pseudomonas aeruginosa*, and *C. crescentus*. In the systems characterized, the *tad* genes are responsible for the biogenesis of Flp (fimbrial low-molecular-weight protein) pili, also known as type IVb subclass pili. Flp-type pili form bundles in *A. actinomycetemcomitans* (25) but exist as individual filaments in *C. crescentus* (23). Flp-type pili are essential for biofilm formation and pathogenesis in several different bacteria (23, 26, 27).

In this study, we report that the *ctp* locus encodes the *A. tumefaciens* common pili and that all of the *ctp* locus genes, with the exception of *ctpF*, are essential for pilus formation. A second unlinked Flp-type pilin gene (*pilA*) can function interchangeably with *ctpA*. Our findings indicate that the Ctp pili contribute to the reversible step of surface interactions and also during maturation of the biofilm. A subset of Ctp pilus mutants, however, are activated to bypass the loss of pili and stimulate reversible surface interactions that require the CtpA pilin but not the Ctp pili.

MATERIALS AND METHODS

Bacterial strains, plasmids, and growth conditions. For the strains and plasmids used in this study, see Table S1 in the supplemental material. The oligonucleotide primers used in this study were obtained from Integrated DNA Technologies (Coralville, IA) (see Table S2 in the supplemental material). All DNA was manipulated by using standard protocols (28). All of the restriction enzymes and molecular biology reagents used were purchased from NEB (Ipswich, MA). DNA sequencing was performed on an ABI 3730 at the Indiana Molecular Biology Institute, Bloomington, IN. DNA was purified with QIAquick Spin kits (Qiagen, Germantown, MD) or E.Z.N.A. Plasmid Miniprep kits (Omega Bio-tek, Norcross, GA) by following the manufacturer's protocols. Plasmid introduction into *A. tumefaciens* was performed via electroporation (29). Bacteria were usually grown on LB medium for *Escherichia coli* or AT minimal medium (30) supplemented with 0.5% (wt/vol) glucose and 15 mM ammonium sulfate (ATGN) medium for *A. tumefaciens*. Sucrose (5%) was used to replace glucose as the sole carbon source (ATSN) during *sacB* counterselection. The following antibiotic concentrations were used: *E. coli*, 100 μg ml^{-1} ampicillin and 25 μg ml^{-1} kanamycin (Km); *A. tumefaciens*, 300 μg ml^{-1} Km. For P_{lac} induction, media were supplemented with isopropyl-β-D-thiogalactopyranoside (IPTG). Unless otherwise noted, reagents, antibiotics, and microbiological media were obtained from Fisher Scientific (Pittsburgh, PA) and Sigma-Aldrich (St. Louis, MO).

Generation of in-frame markerless deletions of *ctp* locus genes, *pilA*, and *uppC*. DNA fragments of approximately 500 bp flanking the targeted gene were generated by PCR. These fragments were located upstream (amplified by primers 3 and 4 [see Table S2 in the supplemental material]) and downstream (amplified by primers 1 and 2 [see Table S2]) of the gene to be deleted and were designed to precisely remove the coding sequence without affecting adjacent genes and to maintain translational coupling for overlapping genes. Primers 2 and 3 were designed with complementary sequences at the 5′ ends to allow splicing by overlapping extension as described previously (7, 31). Briefly, the flanking amplicons were generated with Phusion high-fidelity DNA polymerase (NEB, Ipswich, MA) and agarose gel purified. The purified fragments were used as primers and templates for five cycles of PCR. A final PCR was performed with 1 μl of the flanking amplicons as the template and primers 1 and 4. The resulting amplicon was cloned into pGEM-T Easy and confirmed by DNA sequencing. The fragment was excised with the appropriate restriction enzymes and ligated into the *sacB* counterselectable suicide vector pNPTS138 which had been cleaved with the same enzymes. The vector pNPTS138 (M. R. K. Alley, unpublished data) replicates with a *colE1* origin that is incapable of replicating in *A. tumefaciens* and contains a Km resistance (Km^r) marker and the *sacB* gene, which confers sucrose sensitivity (Suc^s). Derivatives of pNPTS138 were introduced into *A. tumefaciens* by plate mating. The only way for pNPTS138 to confer Km^r on *A. tumefaciens* is recombination into a stable endogenous replicon. Integrants were selected for by growth on ATGN plates supplemented with Km, and plasmid integration was confirmed by PCR, and sucrose sensitivity was confirmed by patching on ATSN. Excision of the integrated plasmid from the Km^r Suc^s clones was facilitated by culturing the recombinants in ATGN without Km overnight twice and then plating them on ATSN. The resulting Suc^r colonies were replica plated on ATGN supplemented with Km to confirm the loss of the plasmid marker. Deletion of the appropriate region of DNA was confirmed by PCR and DNA sequencing.

Creation of complementation constructs. Complementation constructs were prepared by PCR and subsequent cloning of the intact wild-type coding sequences into pSRK-Km or pSRK-Gm (32). The 5′ primers were designed to be cloned into the NdeI site of these vectors (pSRK-Km and pSRK-Gm), directly in frame with the *lacZ*α start codon (see Table S2 in the supplemental material). Coding sequences for *ctpA*, *ctpB*, *ctpE*, and *pilA* were PCR amplified from *A. tumefaciens* C58 genomic DNA with Phusion high-fidelity DNA polymerase and the corresponding primers (primers 7 and 8 for *ctpA*, primers 5 and 6 for *pilA*, *ctpB*, *ctpE*, and *ctpG*). PCR products were gel purified and ligated into pGEM-T Easy. Inserts were confirmed by DNA sequencing. The coding sequences of *ctpA*, *ctpB*, *ctpE*, *ctpG*, and *pilA* were excised by NdeI and HindIII cleavage. All of the excised fragments were ligated with T4 DNA ligase into pSRK-Km(Gm) that had been cleaved with corresponding restriction enzymes. Proper fragment insertion was confirmed by PCR, and constructs were electroporated into *A. tumefaciens* competent cells.

Construction of *lacZ* fusions of upstream and intergenic regions of *ctp* genes and the *pilA* gene. The upstream and intergenic regions of the *ctpA*, *ctpB*, *ctpC*, and *pilA* genes were PCR amplified from *A. tumefaciens* C58 genomic DNA with Phusion high-fidelity DNA polymerase and the corresponding primers (P1 and P2 for *ctpA*, *pilA*, *ctpB*, *ctpC*, and *ctpE* [see Table S2 in the supplemental material]). PCR products were gel purified and ligated into pGEM-T Easy. Inserts were confirmed by DNA sequencing. These DNA fragments were excised and ligated with T4 DNA ligase into pRA301. Proper fragment insertion was confirmed by PCR, and plasmids were electroporated into *A. tumefaciens* competent cells.

β-Galactosidase assay. Cultures were prepared for β-galactosidase assay by culturing in ATGN medium. The optical densities at 600 nm (OD_{600}s) of exponential-phase cultures were measured, and they were frozen at −80°C. β-Galactosidase activity was measured as described previously (33). Briefly, cells were permeabilized in Z-buffer (0.06 M Na_2HPO_4, 0.04 M NaH_2PO_4, 0.01 M KCl, 0.001 M $MgSO_4$, 0.05 M β-mercaptoethanol brought to pH 7.0) by the addition of 2 drops of 0.05% SDS and 4 drops of chloroform. β-Galactosidase reactions were initiated by the addition of 100 μl of a 4-mg/ml solution of the colorimetric substrate *o*-nitrophenyl-β-D-galactopyranoside (ONPG) and terminated by the addition of 600 μl of 1 M $NaCO_2$. Intact cells and debris were removed by centrifugation, free ONPG was determined by measuring the A_{420}, and specific activity was reported in Miller units. At least three biological replicates were performed for each strain at each time point.

Transmission electron microscopy (TEM). Appropriate *A. tumefaciens* C58 derivatives were grown in ATGN minimal medium at 28°C to an OD_{600} of ~1.0 and deposited on carbon-Formvar films on 300-mesh,

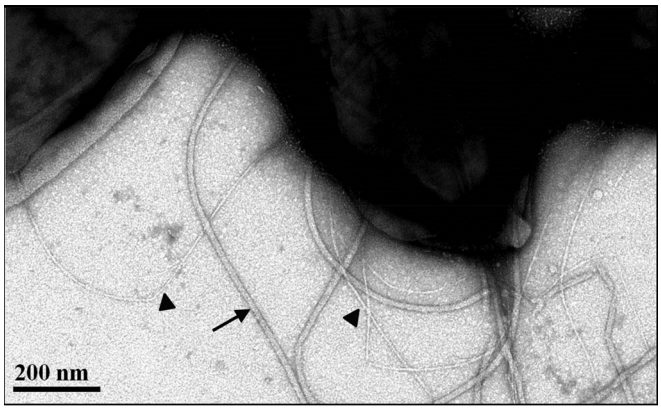

FIG 1 TEM of *A. tumefaciens* C58. Cells were negatively stained with 2% uranyl acetate and visualized by TEM. Arrow, flagellum; filled triangles, common (Ctp) pili.

3-mm copper grids. A 10-μl volume of a bacterial culture was placed on each grid for 1 min, and then the grids were stabilized with glutaraldehyde for 1 min and stained with 2% uranyl acetate for 1 min. The samples were examined with a JEOL JEM-1010 electron microscope at 80 kV in the Indiana University Electron Microscopy Center.

Static-culture biofilm assay. Static-culture biofilms were grown on sterile PVC coverslips suspended vertically in the wells of UV-sterilized 12-well polystyrene dishes. Cell cultures were adjusted to an OD_{600} of 0.05, inoculated into 3 ml of ATGN broth, and then incubated at room temperature for 24 to 72 h. Adherence to PVC coverslips was visualized by staining of rinsed coverslips with 1% crystal violet (CV) for 10 min at room temperature. Quantification of adherent biomass was achieved via solubilization of adsorbed CV in 1 ml of 33% acetic acid. Solubilized CV was measured by determining the A_{600} to estimate relative amounts of adhered biomass and normalized to the planktonic culture density (OD_{600}).

Short-term binding assay with UPP staining. Short-term binding assays were conducted by growing cell cultures to an OD_{600} of ~0.6. Glass coverslips were placed at the bottom of 2 ml cell culture volumes in 3-ml petri plates for 1 h. Coverslips were removed from the plates, rinsed with water three times for 10 min per rinse. Fluorescent Alexa fluor 594-conjugated wheat germ agglutinin (af-WGA; Invitrogen) at 0.01 mg/ml was then added as a 100-μl pool to one side of the coverslip lying flat, incubated for 30 min, washed thoroughly with water, and mounted on slides for microscopy. Bright-field and epifluorescence microscopy was performed on a Nikon E800 at ×100 magnification. Epifluorescence microscopy used a G-2B filter set (excitation filter, 510 to 560 nm; dichromatic mirror, 575 nm; emission filter, 610 nm). Each strain was tested in triplicate, and fields were analyzed randomly. Cell numbers and lectin labeling were counted manually or automatically with the ImageJ program (NIH).

Plant root binding assay. An attachment assay with *Arabidopsis thaliana* ecotype WS used 7- to 10-day-old seedlings grown from seeds surface sterilized with ethanol and planted on half-strength Murashige-Skoog agar medium (34, 35). Roots were cut into 1-cm segments and rinsed in sterile dishes containing 2 ml of 1 mM $CaCl_2$ and 0.4% sucrose and then inoculated with cell suspensions of *A. tumefaciens* (OD_{600} of ~0.01). The appropriate derivative strains of *A. tumefaciens* C58 used in this assay carried a green fluorescent protein reporter construct under constitutive expression (P_{tac}-*gfpmut3*, pJZ383). Four root segments were inoculated per strain. After 48 h of incubation in the dark at room temperature, the root segments were recovered, rinsed and resuspended in fresh calcium chloride-sucrose solution, and sealed under coverslips for hydration. Microscopy was performed with a Nikon A1 confocal microscope at ×60 magnification with a 488-nm laser for excitation and a 500- to 550-nm filter for emission. Images were acquired and analyzed with the Elements software package.

Potato disk tumor assay. The virulence potential of each strain was evaluated by monitoring the ability to initiate tumor formation on red potato slices (34, 35). One-centimeter-diameter cores were obtained from organic red potatoes that had been washed in distilled water, incubated for 20 min in 10% bleach, and UV irradiated for 20 min. Disks were sliced (0.5 cm) from the center portion of individual cores and placed onto 1.5% agar plates with no additional nutritional supplementation. Overnight cultures of the strains indicated were diluted to an OD_{600} of 0.6 in ATGN and serially diluted 10- and 100-fold. A 50-μl volume of each dilution were inoculated onto the potato surface and allowed to be absorbed. Plates were sealed with Parafilm and incubated undisturbed for 4 weeks at room temperature. Tumors were enumerated on days 14, 21, and 28. Each strain was tested in three independent experiments containing five technical replicates per experiment per inoculum.

Flow cell biofilm assay. Flow cell biofilms were cultured as described previously (4). Once-through flow cells were purchased through the Technical University of Denmark and inoculated with diluted overnight cultures (100 μl per flow chamber, final OD_{600} of 0.05). After inoculation, cells were permitted to attach for 60 min before the flow of ATGN medium with appropriate antibiotics commenced at ~3 ml/h. Each strain harbored the pJZ383 (P_{tac}-*gfpmut3*) plasmid and was inoculated into triplicate chambers. Growing biofilms were examined by confocal microscopy at 24-h intervals for 1 to 5 days postinoculation. Microscopy was performed with a Nikon A1 scanning laser confocal microscope at ×60 magnification with a 488-nm laser for excitation and a 500- to 550-nm filter for emission. Images were acquired with the Elements software package and analyzed with an automated version of the biofilm analysis software COMSTAT (36) called autoCOMSTAT running in MATLAB 2013 (7).

RESULTS

The *ctp* genes are similar to the *tad* type IVb pilus assembly locus. Common pili are readily identified by TEM analysis of *A. tumefaciens* C58 (Fig. 1), but their genetic basis had not been established. The *A. tumefaciens ctpABCDEFGHI* (cluster of type IV pili, Atu0216 to Atu0224) locus on the C58 circular chromosome was highly homologous to the *tad*-type locus from *A. actinomycetemcomitans* (Table 1) (24, 37). The *tad* locus has 14 genes, including 2 pilin genes, 2 pseudopilin genes, 1 peptidase gene, and 9 pilus biogenesis and basal body genes. The *ctp* locus in *A. tumefaciens* C58 contains one gene that encodes a 63-amino-acid (aa) protein homologous to pilin (*ctpA*), one presumptive pilin peptidase gene

TABLE 1 Percent sequence identities between the products of the *ctp* gene of *A. tumefaciens*, the *cpa* gene of *C. crescentus*, and the *tad* gene of *A. actinomycetemcomitans* and promoter activities of intergenic regions in the *ctp* cluster

A. tumefaciens ctp product	*C. crescentus cpa* product (% identity)[a]	*A. actinomycetemcomitans tad* product (% identity)[a]	Promoter activity[b]
CtpA	PilA (55.9)	Flp-1 (24.2), Flp-2 (23.4)	2,099.8 ± 224.5
PilA	PilA (30.4)	Flp-1 (23.9), Flp-2 (28.8)	<1.0
CtpB	CpaA (34.1)	TadV (22.0)	8.3 ± 4.2
CtpC	CpaB (32.0)	RcpC (17.6)	10.2 ± 1.1
CtpD	CpaC (30.9)	RcpA (23.5)	NA
CtpE	CpaD (27.1)	RcpB (11.2)	77.4 ± 7.5
CtpF	CpaE (43.9)	TadZ (15.3)	NA
CtpG	CpaF (67.3)	TadA (45.7)	NA
CtpH		TadB (21.7)	NA
CtpI		TadC (16.7)	NA

[a] Protein sequence alignment was performed by the ClustalW method with the Lasergene software.
[b] Values are in Miller units. NA, not assayed.

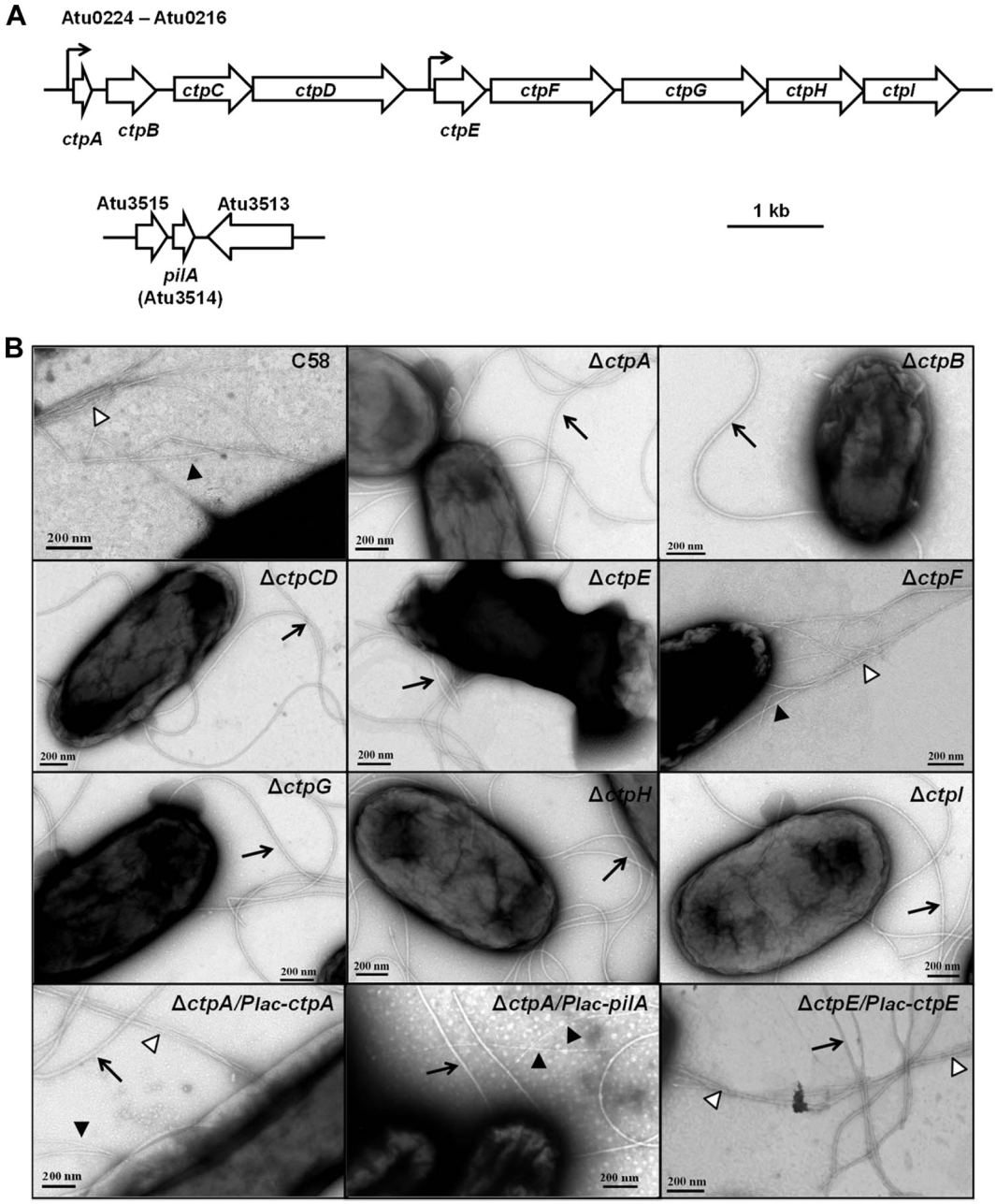

FIG 2 *ctp* genes encode the production of common pili. (A) Gene maps of the *ctp* cluster and the unlinked *pilA* gene (Atu3514). The *ctp* cluster contained nine genes (Atu0216 to Atu0224). Arrows indicate promoters in the *ctp* cluster. (B) TEM of *A. tumefaciens* C58, *ctp* mutants, and complemented derivatives. Arrows, flagella; filled triangles, Ctp pili; open triangles, Ctp pilus bundles. Cells were negatively stained with uranyl acetate and visualized by TEM.

(*ctpB*), and seven additional genes (*ctpCDEFGHI*) predicted to make up the pilus assembly and basal body complex (Table 1) (Fig. 2A). The *A. tumefaciens ctp* gene cluster is also highly homologous to the *cpa* locus in *C. crescentus*, which encodes the Cpa pili (Table 1) (24). Orthologous genes in the *ctp*, *tad*, and *cpa* clusters were syntenous, with pairwise amino acid sequence identities of 20 to 60% (Table 1). In addition, there is another gene that encodes a 71-aa protein, is similar to *ctpA*, is designated *pilA* (Atu3514, Fig. 2A), and is located on the linear chromosome but is not associated with other *tad*-type genes. The upstream and intergenic regions of several *ctp* genes and *pilA* were used to create plasmid-borne *lacZ* translational fusions, and putative promoter activities were identified upstream of the *ctpA* and *ctpE* genes (Table 1) (Fig. 2A).

The Flp pilin components are a unique subclass within the type IVb pilin family and have several novel features (38). First, the Flp prepilin proteins usually vary from 50 to 80 aa. Second, the signal peptides in Flp prepilin have variable lengths of 10 to 26 aa. Third, a highly conserved "Flp motif" (G/XXXXEY) is situated in the hydrophobic N-terminal domain and is the site at which the prepilin peptidase cleavage generates the mature pilin. Finally, no cysteine residues exist in the Flp prepilin protein. Both CtpA and

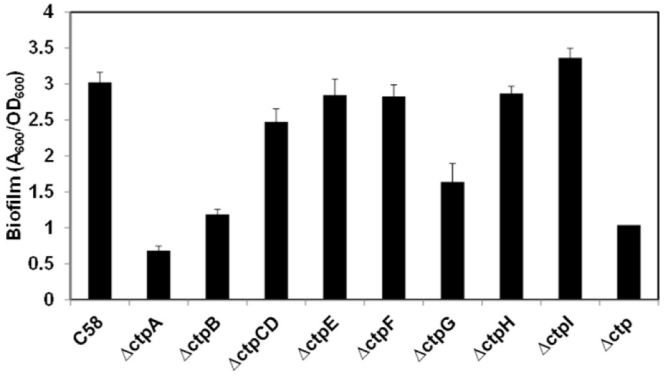

FIG 3 Biofilm formation by *A. tumefaciens ctp* deletion mutants. Static biofilms of *A. tumefaciens* C58 and all *ctp* mutants were incubated for 72 h on coverslips. All bacterial strains grown in shaking liquid culture overnight were diluted to an OD_{600} of 0.05 and incubated in 12-well plates with PVC coverslips for 72 h at 28°C. After rinsing, coverslips were stained with 1% CV and the adherent biomass was quantified by measuring the absorbance of acetic acid-solubilized CV, normalized for planktonic culture growth (A_{600}/OD_{600}). Error bars show standard deviations of results of assays performed in triplicate.

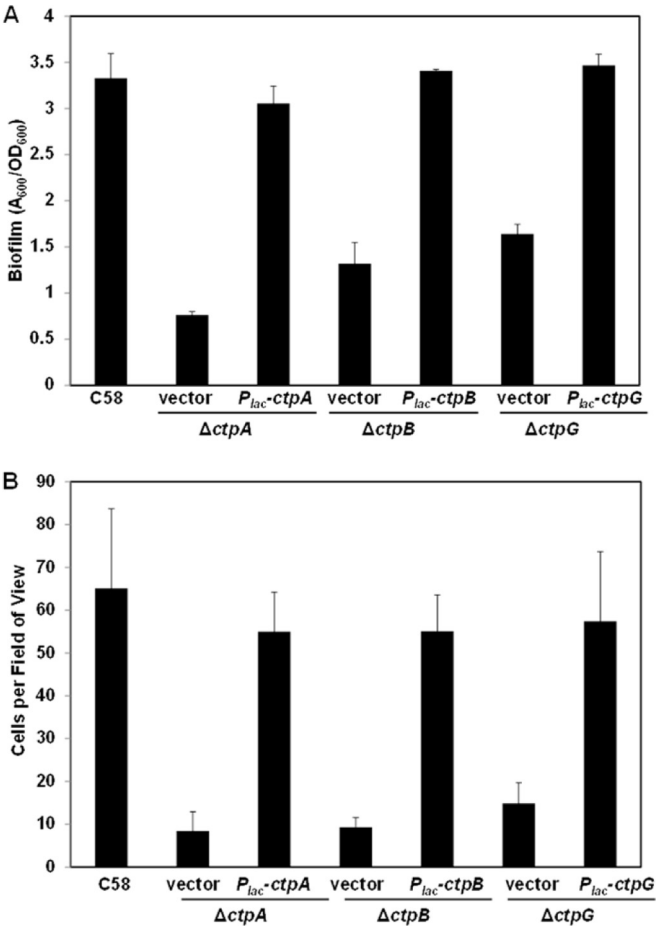

FIG 4 Complementation of class I Ctp mutants. *A. tumefaciens* mutants were complemented by plasmid-borne, ectopically expressed constructs (P_{lac}-*ctpA*, P_{lac}-*ctpB*, and P_{lac}-*ctpG*). (A) Seventy-two-hour static biofilm assays on coverslips prepared as described in the legend to Fig. 3 and grown with 500 μM IPTG induction. (B) Short-term irreversible binding assays on coverslips with 500 μM IPTG induction. Coverslips were incubated with cell culture for 1 h and then subjected to strong washing. Total numbers of attached cells per field of view ($\sim 3.13 \times 10^4$ μm^2) were determined by counting with a Nikon E800 in bright-field mode at ×100 magnification. The values are mean results of 10 fields of view, and the error bars show the standard deviations.

PilA from *A. tumefaciens* exhibit these Flp-pilin features, and thus, we hypothesized that they could each function to form Flp pili.

The *ctp* genes encode the common pili. Two types of filaments on the cell surface were observed in the wild-type C58 strain under TEM (Fig. 1). The thicker (18- to 20-nm) and more curved filaments were flagella (Fig. 2B, arrows). The other filaments observed were much thinner (~3 nm thick) and straighter (Fig. 2B, filled triangles), sometimes in large bundles (Fig. 2B, open triangles; see C58 panel for an example). These are similar in size and character to the common pili reported previously (20). In-frame deletions of each *ctp* gene were constructed in *A. tumefaciens* C58. The common pili were absent from a TEM analysis of all of the *ctp* mutants, except the Δ*ctpF* mutant (Fig. 2B). In addition, IPTG-controlled expression of plasmid-borne *ctpA* and *ctpE* could complement the nonpiliated phenotypes of the Δ*ctpA* and Δ*ctpE* mutants, respectively (Fig. 2B). These results indicate that the *ctp* locus is required for elaboration of the common pili, and they are likely to be composed of the CtpA pilin.

A subset of *ctp* genes is required for biofilm formation. The in-frame deletion mutants were examined for biofilm formation on coverslips under static conditions (Fig. 3). According to their biofilm phenotypes, *ctp* mutants were divided into two categories. The Δ*ctpA*, Δ*ctpB*, and Δ*ctpG* mutants were all significantly deficient in biofilm formation. Both the Δ*ctpA* and Δ*ctpB* mutants showed depressed biofilm formation during the entire experiment, whereas the Δ*ctpG* mutant was similar to the wild type in the early stages (12 h) but manifested significantly decreased biofilm formation from 24 to 72 h (see Fig. S1 in the supplemental material). These biofilm-deficient mutants were all designated class I mutants. However, other *ctp* gene cluster mutants, including the Δ*ctpCD*, Δ*ctpE*, Δ*ctpF*, Δ*ctpH*, and Δ*ctpI* mutants, were equivalent to the wild type in biofilm formation (Fig. 3). This was surprising, as our TEM results indicated that the Δ*ctpCD*, Δ*ctpE*, Δ*ctpH*, and Δ*ctpI* mutants do not produce pili under standard growth conditions (Fig. 2B; the Δ*ctpF* mutation affected neither pilus formation nor biofilm formation). The *ctp* genes that did not impact biofilm formation were designated class II genes. To evaluate the relationship between class I and II *ctp* genes, the entire *ctp* locus (Δ*ctp*, Atu0216 to Atu0224) was deleted. The Δ*ctp* mutant phenotype was indistinguishable from that of the class I mutants (Fig. 3).

The biofilm deficiencies of class I mutants were complemented by plasmid-borne expression of the corresponding genes under P_{lac} promoter control induced with IPTG (Fig. 4A), confirming the roles of these individual genes. The *ctpA* gene encodes the prepilin subunit protein, *ctpB* encodes a peptidase that presumptively processes the prepilin, and *ctpG* encodes an ATPase, predicted to be cytoplasmic and to provide the energy for pilus assembly (38, 39). Moreover, ectopic expression of *ctpA* was unable to suppress the biofilm and short-term attachment deficiency of the Δ*ctpB* mutant (see Fig. S2B in the supplemental material), suggesting that CtpA prepilin was not functional until processed by CtpB.

A second pilin homologue can function in the place of *ctpA*. In addition to the *ctp* cluster located on the circular chromosome, another Flp-type pilin is located on the linear chromosome and

annotated as *pilA* (Atu3514, Fig. 2A). There are no additional *tad*-like genes adjacent to *pilA*. The N-terminal hydrophobic segments of PilA and CtpA are highly similar, and PilA has the well-conserved Flp motif G/ATAIEY (24). These features suggested that CtpA and PilA might have similar functions. In-frame deletion of *pilA* did not produce any decrease in biofilm formation, and overexpression of *pilA* in the wild type did not increase biofilm formation (see Fig. S2 in the supplemental material). The Δ*ctpA* Δ*pilA* double pilin deletion mutant exhibited a biofilm deficiency similar to that of the Δ*ctpA* single mutant. Strikingly, however, overexpression of a plasmid-borne *pilA* gene from P_{lac} in the Δ*ctpA* mutant could effectively complement the deficiency in biofilm formation and pilus production in the Δ*ctpA* mutant (Fig. 2B; see Fig. S2A in the supplemental material). As with *ctpA*, ectopic expression of *pilA* had no effect in a *ctpB* mutant, suggesting that CtpB is also required to process PilA (see Fig. S2B). Moreover, the promoter activity of the *pilA* gene upstream region was negligible under standard culture conditions (Table 1), suggesting that the *pilA* gene is not expressed under minimal-medium standard culture conditions.

Class I *ctp* genes function in cell-to-surface attachment and also promote biofilm maturation. We examined the early stages of surface association of the class I *ctp* mutants. A short-term binding assay was performed with the class I mutants and their complemented derivatives to evaluate the proficiency of their attachment to abiotic surfaces. The three class I mutants displayed pronounced short-term binding deficiencies, and the plasmid-borne copies of the corresponding genes complemented these defects (Fig. 4B).

Furthermore, careful comparison of biofilm formation by the wild type and mutants over time revealed a role for the class I *ctp* gene products in biofilm maturation. Four linear regression models were fitted to biofilm formation (A_{600}) relative to days of incubation, with P values of <0.05 (see Fig. S3 in the supplemental material). This analysis reflected a linear correlation between incubation time and biofilm formation. With linear regression models, the amount of biofilm formed at 12 h (A_{600}) for the wild-type strain was 0.49, greater than that of the *ctpA* mutant (0.23), the *ctpB* mutant (0.18), and the *ctpG* mutant (0.36), consistent with the surface attachment deficiency of these mutants. In addition, the slopes of linear biofilm accumulation (A_{600}/h), which are indicative of the rate of biomass accumulation in the biofilm, were also significantly greater for the wild-type strain, at 0.77 (A_{600}/h), than for the class I mutants (Δ*ctpA*, 0.11; Δ*ctpB*, 0.28; Δ*ctpG*, 0.35).

Deficiencies in biofilm formation under flowing conditions. We compared the biofilm formation of wild-type C58 and the Δ*ctpA* Δ*pilA* double mutant in flow cell chambers under low-shear conditions in which the growing biofilms were continuously washed with fresh medium. As we knew that, when expressed, *pilA* can function in place of *ctpA*, we used the double pilin mutant to ensure that the mutant would be nonpiliated regardless of the culture conditions. CSLM analysis of biofilms with derivatives constitutively expressing *gfp* revealed that, similar to the biofilm deficiency observed in static assays, the Δ*ctpA* Δ*pilA* double mutant had clearly diminished biofilm formation relative to that of the wild type (Fig. 5). As has been documented previously (4), wild-type C58 developed extensive biofilms and formed large, tall (up to 30 μm) microcolonies (Fig. 5A), whereas the Δ*ctpA* Δ*pilA* mutant biofilms were sparse with small cell aggregates (Fig. 5B). We examined the confocal image data with an automated version of the COMSTAT biofilm analysis program, autoCOMSTAT (7) to quantitatively analyze the biofilm structure. The Δ*ctpA* Δ*pilA* mutant had a lower biovolume than the wild type during the entire incubation period (Fig. 5C). Early on, the average heights of the mutant and wild-type biofilms were similar but the wild-type biofilms then increased rapidly and eventually became three times as high as the mutant biofilms (Fig. 5D).

Biofilm formation on plant roots and tumor formation on potato disks. We also qualitatively examined binding to *A. thaliana* root segments suspended in a nonnutritive buffered medium. No consistent difference between the 48-h biofilms formed on plant roots by the Δ*ctpA* mutant and the wild type was observed (see Fig. S4A in the supplemental material). These data suggested that lack of Ctp pili does not cause a significant deficiency in mature biofilm formation on plant roots. However, this method is nonquantitative and provides only a rough measurement of the bacterium-plant interaction, so subtle differences in surface interactions, such as those manifested by the nonpiliated class I mutants, may not be distinguishable.

Moreover, we examined the virulence of *ctp* mutants. The Δ*ctpA* (class I) and Δ*ctpCD* (class II) mutants were virulent and caused tumor formation in potato disks, with no obvious differences from the wild-type strain in tumor quantity or size (see Fig. S4B in the supplemental material).

Class II *ctp* mutants are not rescued by other pilin secretion systems but have elevated reversible cell-to-surface attachment. It was surprising that although class II mutants formed biofilms that were similar to those of the wild type, they did not produce common pili detectable by TEM. These class II *ctp* genes (*ctpCDE* and *ctpGHI*) are predicted to make up the basal body of the Ctp pilus, based on homology to other *tad* systems (24). It seemed plausible that pilin subunits might be secreted out of the cell through the secretion systems of other pilus types. As mentioned earlier, only the conjugal pili for the pAtC58 plasmid are expected to be produced under standard laboratory conditions (the Ti plasmid T pilus and the plasmid's conjugal pili are both under tight regulation), but it was formally possible that the pAtC58 *avhB* secretion system or the others might function in the absence of the class II *ctp* genes (16, 20). Class II mutants were therefore created in the C58p$^-$ strain, a derivative cured of the At and Ti plasmids (40). No difference between the C58p$^-$ strain and its class II mutants was observed (see Fig. S5 in the supplemental material), excluding the possibility that that pilin subunits were secreted through these plasmid-borne pilus systems.

In addition to mature biofilm formation, we also tested the short-term bacterium-to-surface attachment of class II mutants. *A. tumefaciens* produces a UPP that is crucial for irreversible bacterial attachment to surfaces (41). The UPP is produced upon surface contact, and it is rarely made by free-swimming cells (42). Bacterium-to-surface attachment and UPP production within 1 h by the wild type and the class II mutants were compared (Fig. 6). Intriguingly, the class II mutants all exhibited greater short-term binding and a greater proportion of cells producing the UPP in 1 h than the wild type.

There are two hypotheses that might explain the enhanced short-term binding of class II *ctp* mutants. (i) These mutants have greater reversible bacterium-to-surface attachment, resulting in more uniform deployment of the UPP in the colonizing popula-

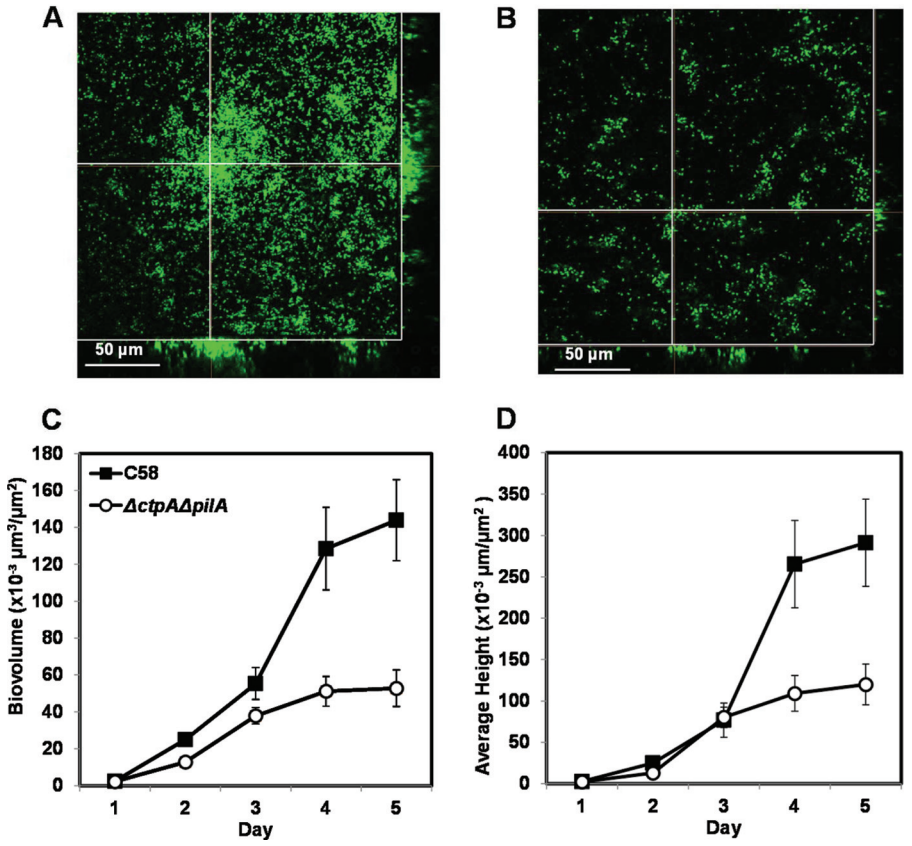

FIG 5 Flow cell biofilms of wild-type C58 and a Δ*ctpA* Δ*pilA* double mutant. SCLM images of flow cell biofilms formed by wild-type C58 (A) and the Δ*ctpA* Δ*pilA* double mutant (B) each harboring a P_{tac}-*gfpmut3* plasmid (pJZ383) after 5 days of incubation with a Nikon A1 SCLM with a 488-nm laser for excitation and a 500- to 550-nm filter for emission. The crossed lines in each image indicate the positions of the sagittal, three-dimensional reconstructions in the side bars. The error bars show the standard errors of the means. The images were rendered with the Nikon Elements software package. The autoCOMSTAT program was used to calculate the biovolume per substratum area (C) and average biofilm height per substratum area (D). The values are averages calculated for 12 to 15 image stacks collected from three channels for each strain per time point.

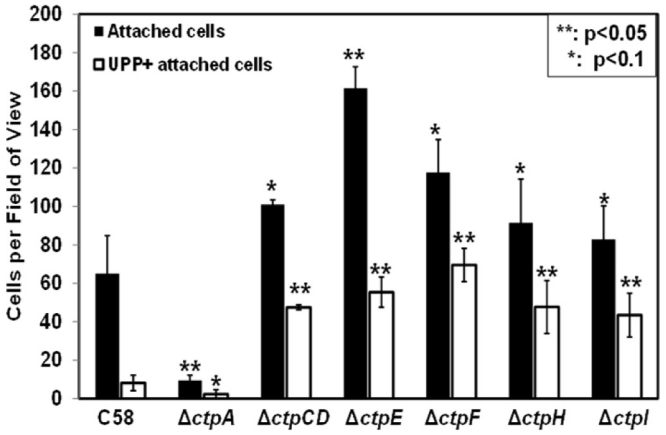

FIG 6 Irreversible attachment of class II Ctp mutants: Coverslips were incubated with cell cultures for 1 h, subjected to robust rinsing, stained with af-WGA for 30 min, and then vigorously rinsed again. The total numbers of attached cells per field of view (~3.13×10^4 μm^2) were determined with a Nikon E800 at ×100 magnification in bright-field mode. Enumeration of UPPs was done by determining the number of af-WGA-stained red fluorescent dots by fluorescence microscopy. The values are mean results of 10 fields of view, and the error bars show the standard deviations.

tion. (ii) These mutants have more elevated UPP production in planktonic cells, leading to more stable bacterial engagement with the surface. *uppC*, a UPP biosynthetic gene required for polysaccharide production (Atu1238; which encodes a Wza outer membrane porin for polysaccharide export), was deleted from all of the class II mutants. These mutants cannot produce the UPP but clearly are much more effective at reversible attachment than the Δ*uppC* single mutant alone is (Fig. 7; see Fig. S6 in the supplemental material). Mutants with the Δ*uppC* deletion were readily removed from the surface by washing, whereas the wild type was stably attached. These results are consistent with the hypothesis that class II mutants have enhanced reversible bacterium-to-surface interactions.

The *ctpA* mutation is epistatic over class II *ctp* mutants. The class II mutants still express the other components of the Ctp pilus, including the *ctpA* pilin and its presumptive peptidase *ctpB*. It seemed likely that the class II mutants, which do not make visible pili and have enhanced reversible surface binding and robust biofilm formation, would be independent of the CtpA pilin. The Δ*ctpA* in-frame deletion was constructed in all of the class II mutants. Surprisingly, the Δ*ctpA* class II double mutants had a biofilm-deficient phenotype similar to that of the Δ*ctpA* single mutant (Fig. 8). Moreover, deletion of *ctpA* from class II mutants abolished their elevated short-term binding, suggesting that the

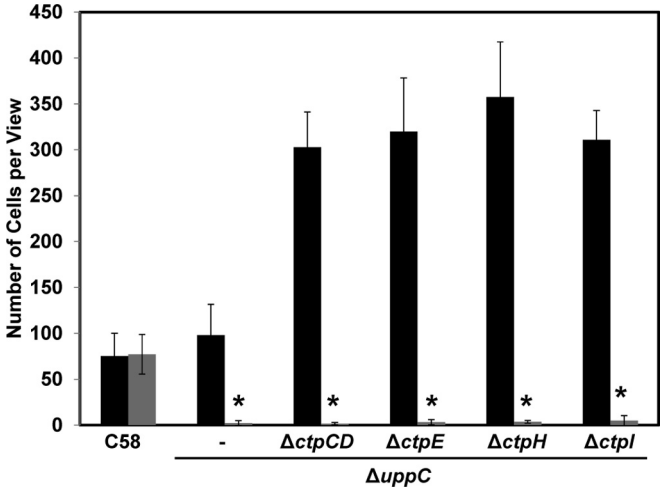

FIG 7 Comparison of reversible and stable surface attachment. Short-term binding assays were performed with *A. tumefaciens* C58 and Δ*uppC* single and Δ*uppC*/class II Ctp double mutants. Coverslips were incubated with cell culture for 1 h and then minimally rinsed (black bars, total numbers of reversible attached cells) or vigorously rinsed (gray bars, total numbers of irreversibly attached cells). Total numbers of attached cells per field of view (~3.13×10^4 μm^2) were determined with a Nikon E800 in bright-field mode at ×100 magnification. The values are mean results of 10 fields of view, and the error bars show the standard deviations. Asterisks show that attached cells were rarely observed.

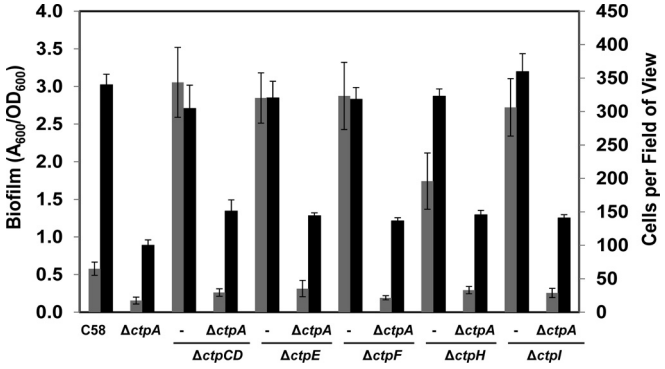

FIG 8 The *ctpA* mutation is epistatic to class II Ctp mutants. Static biofilm formation and stable short-term surface attachment of C58 and Δ*ctpA*, class II, and Δ*ctpA*/class II Ctp mutants were measured. Gray bars are the total numbers of irreversible attached cells per field of view (~3.13×10^4 μm^2) from short-term binding assays viewed with a Nikon E800 at ×100 magnification in bright-field mode. The values are mean values of 10 fields of view, and the error bars show the standard deviations of the means. Black bars are quantifications of acetic acid-solubilized CV on 72-h coverslip biofilms. Adherent biomass was normalized by growth (A_{600}/OD_{600}), and error bars are standard deviations of results of assays run in triplicate.

class II mutants still require the CtpA pilin, even though this protein is not assembled into a visible pilus structure.

DISCUSSION

The common pili of *A. tumefaciens* have been observed by electron microscopy in previous studies (20). In this study, we have provided evidence that the *ctpABCDEFGHI* locus (Atu0216 to Atu0224) encodes the production of these common pili and that all of the genes except for *ctpF* are required to generate the filaments. As with other members of the type IVb pilus subfamily (24), we have found that the Ctp common pili of *A. tumefaciens* contribute to attachment and biofilm formation. Nonpiliated class I Ctp mutants manifest a consistent and significant deficiency in reversible surface interactions and biofilm formation, although these mutants are not completely deficient. Our observations are consistent with the adhesion phenotype of mutants in the related Cpa pilus from *C. crescentus*, in which mutants show decreased attachment but are not completely blocked (15). In contrast, *tad* mutants of *A. actinomycetemcomitans* have a dramatic loss of attachment, aggregation, and biofilm formation (37, 39). Our findings suggest that in *A. tumefaciens*, the Ctp pili enhance reversible surface interactions but are not absolutely required for attachment (Fig. 2 and 3). It seems likely that these pili promote initial interactions that eventually result in stable attachment and biofilm formation. As biofilms mature, this activity appears to contribute to cell-cell interactions.

Tad-type pilus systems and the *A. tumefaciens* Ctp cluster. The *A. actinomycetemcomitans* Flp pili were the first discovered type IVb pili and remain the most thoroughly studied (25). In *A. actinomycetemcomitans*, the *tad* locus is responsible for the assembly and secretion of the Flp pili. Adherent strains of *A. actinomycetemcomitans* form copious, long, thick, and bundled Flp pilus fibrils; show a wrinkled colony morphology; form autoaggregates that are difficult to disperse; and tenaciously form biofilms on solid surfaces (27). *A. actinomycetemcomitans* derivatives that cannot form Flp pili are nonadherent and nonaggregating and produce smooth colonies. In contrast, wild-type *A. tumefaciens* C58 forms a limited number of Ctp pilus fibrils, has a smooth colony morphology, and aggregates only modestly. The Ctp pili observed by TEM in *A. tumefaciens* strains were often unbundled and distributed around the cell body. Additional cells and other pili were often observed bound at the tips of the fibers, consistent with their role in attachment and reversible surface interactions. Sporadically, we also observed thick Ctp pilus bundles (indicated by the open triangles in TEM images of the C58 strain in Fig. 2B). Thus, the Ctp pili might also associate to form a matrix of thick, bundled fibrils, binding along their length to bacterial cell surfaces to promote cell accumulation during biofilm maturation. These two hypothesized functions of Ctp pili agree with our results that the Ctp pili function both in reversible cell-to-surface short-term binding at early stages of surface interaction and in late biofilm maturation.

The *tad* locus in *A. actinomycetemcomitans* contains 14 genes, *flp-1*, *flp-2*, *tadV*, *rcpCAB*, and *tadZABCDEFG*, and independent mutations in these genes caused a nonadherence phenotype and the loss of Flp pilus production in *A. actinomycetemcomitans* (37, 39). Similar *tad* loci are found in the genomes of a wide variety of Gram-negative and Gram-positive bacteria (24). In *C. crescentus*, the Cpa locus contains nine genes that are required for production of the polar Cpa pili that function in adhesion, although other genes may be required as well (23). The Cpa locus is nearly gene-for-gene homologous and syntenous with the Ctp-encoding genes in *A. tumefaciens*. We determined that all of the *A. tumefaciens ctp* genes were required for elaboration of Ctp pili, except *ctpF* and the unlinked *pilA* gene that is homologous to *ctpA*.

The *ctpF* gene was not required for pilus formation, and the *ctpF* mutant did not influence adherence. The location of *ctpF* in the middle of the gene cluster (Fig. 2A) suggests that it should be coexpressed with the other *ctp* genes. In the *C. crescentus cpa* gene

cluster, the *cpaE* gene is homologous to *ctpF* (23). CpaE is thought to be required for unipolar localization of pili in *C. crescentus*. However, the Ctp common pili in *A. tumefaciens* are distributed over the entire cell body. The CtpF protein must therefore perform some other function in *A. tumefaciens* that is not fundamentally required for pilus production under laboratory conditions or it is not functional.

The adherence of the *pilA* mutant was also unaffected, but the ectopic expression of *pilA* from a plasmid rescued the adherence defect of the *ctpA* mutant. Although it encodes a protein that is highly similar to the CtpA prepilin, the *pilA* gene is located on the linear chromosome rather than the circular chromosome on which the *ctp* locus resides and there are no other *tad*-type genes on this replicon. These observations suggest that PilA alone can function as a pilin subunit, productively interacting with the Ctp pilus assembly components, but that it may not be fully expressed under laboratory conditions. The plasmid-borne allele expresses *pilA* from the strong P_{lac} promoter and fuses the start codon of the gene to the efficient *lacZ* Shine-Dalgarno sequence for translation. It remains unclear why this separate and apparently functional prepilin gene is maintained in the *A. tumefaciens* genome.

The *ctpA* pilin and other class I Ctp genes. Deletion of *ctpA*, the major pilin subunit gene in *A. tumefaciens* C58, resulted in a moderate decrease in biofilm formation, an approximately 50% reduction relative to that of the wild type. It seems that the Ctp pili do not play as crucial a role in the adherence-related phenotypes of *A. tumefaciens* as they do in *A. actinomycetemcomitans*. It is possible that under laboratory conditions, the *ctp* pili are not fully expressed. These pili may play a more important role in bacterial attachment under other environmental conditions that lead to more active pilus production. However, as yet, no such conditions that clearly stimulate Ctp pilus elaboration in *A. tumefaciens* have been identified.

The *ctpB* gene encodes a homologue of the prepilin peptidase (e.g., TadV) thought to process the Flp-type prepilin to its mature form, by cleaving them at conserved glycine residues at the G/XXXXEY motif in the prepilin N terminus (43). Given that the *ctpB* deletion mutant has the same level of adhesion defect as the *ctpA* mutant and overexpression of neither *ctpA* nor *pilA* could suppress the Δ*ctpB* mutant biofilm deficiency, it seems highly likely that *ctpB* recognizes and processes the CtpA prepilin. Likewise, it must be capable of processing the PilA protein. Despite limited overall homology between the CtpA and PilA proteins, they both have the G/XXXXEY motif and the sequence is the same (G/ATAIEY, positions 14 to 20 in CtpA and 29 to 35 in PilA).

Interestingly the *ctpG* mutant manifests an adhesion deficiency (class I) whereas those with mutations in the other *ctp* genes flanking it do not (class II). *ctpG* encodes a predicted ATPase homologous to TadA and CpaF with Walker A and B motifs, proteins required to energize pilus assembly (44). The *ctpG* mutant is clearly nonpiliated and does manifest an adhesion deficiency consistent with the *ctpA* and *ctpB* mutants. Its inability to assemble pili is likely responsible for this defect. Whatever CtpA-dependent mechanism allows the class II mutants to attach efficiently despite the absence of common pili, this either must not be engaged in the *ctpG* mutant or may require functional CtpG (see below).

Class II Ctp-encoding genes are dispensable for adherence but require the CtpA pilin. The *ctp* locus contains only nine genes and lacks homologues of the *tadDEFG* genes (24). Most of the *tad* genes are required for adherence in *A. actinomycetemcomitans*, but in *A. tumefaciens*, deletion of only the class I gene *ctpA*, *ctpB*, or *ctpG* caused decreases in attachment and biofilm formation. Mutations of the class II genes *ctpCD*, *ctpE*, *ctpG*, *ctpH*, and *ctpI* resulted in strains that did not produce pili but were not diminished in adherence and even seemed to accelerate reversible surface attachment. This adherence, however, remained dependent upon *ctpA*. Thus, it seems that the Ctp pilin subunits can function in an unexpected way, in which they promote adherence even in the absence of the Ctp pili.

Two models seem plausible to explain the class II mutant attachment phenotype. In the first, mature pilin subunits accumulate in the periplasm of class II mutants. In the absence of the remaining pilus biogenesis functions, the accumulated pilin proteins in the periplasm become jammed in one or more export systems. These jammed pilins function as independent adhesins in bacterial attachment, which could compensate for the attachment deficiency due to the lack of pilus formation. The second model still invokes the accumulation of pilins in the periplasm, but in this model, the adherence phenotype is influenced by envelope stress that triggers increased adhesion via other mechanisms and compensates for the lack of pili. This stress response might activate specific downstream regulatory systems that promote cell-to-surface attachment and biofilm formation that is independent of the Ctp pili and does not directly involve CtpA pilin. It could be that this envelope stress requires the presumptive CtpG ATPase since it is required for normal attachment and does not bypass the requirement for pili. CtpG may have a role in the accumulation of CtpA in the periplasm in class II Ctp mutants. These two models are not mutually exclusive, and the observed phenotype of class II Ctp mutants may result from a combination of both processes.

ACKNOWLEDGMENTS

This project was supported by National Institutes of Health (NIH) grant GM080546 to C.F.

We thank Y. V. Brun, M. E. Winkler, and D. B. Kearns for helpful input and suggestions, as well as Fuqua lab members for extensive discussions. We also acknowledge assistance from the IUB Light Microscopy Imaging Center and the IU Electron Microscopy Center.

REFERENCES

1. **Chilton MD, Drummond MH, Merio DJ, Sciaky D, Montoya AL, Gordon MP, Nester EW.** 1977. Stable incorporation of plasmid DNA into higher plant cells: the molecular basis of crown gall tumorigenesis. Cell **11:**263–271. http://dx.doi.org/10.1016/0092-8674(77)90043-5.
2. **Moore LW, Chilton WS, Canfield ML.** 1997. Diversity of opines and opine-catabolizing bacteria isolated from naturally occurring crown gall tumors. Appl. Environ. Microbiol. **63:**201–207.
3. **Danhorn T, Hentzer M, Givskov M, Parsek MR, Fuqua C.** 2004. Phosphorus limitation enhances biofilm formation of the plant pathogen *Agrobacterium tumefaciens* through the PhoR-PhoB regulatory system. J. Bacteriol. **186:**4492–4501. http://dx.doi.org/10.1128/JB.186.14.4492-4501.2004.
4. **Ramey BE, Matthysse AG, Fuqua C.** 2004. The FNR-type transcriptional regulator SinR controls maturation of *Agrobacterium tumefaciens* biofilms. Mol. Microbiol. **52:**1495–1511. http://dx.doi.org/10.1111/j.1365-2958.2004.04079.x.
5. **Heindl J, Wang Y, Heckel BC, Mohari B, Feirer N, Fuqua C.** 2014. Mechanisms and regulation of surface interactions and biofilm formation in Agrobacterium. Front. Plant Sci. **5:**176. http://dx.doi.org/10.3389/fpls.2014.00176.
6. **Ashby AM, Watson MD, Loake GJ, Shaw CH.** 1988. Ti plasmid-specified chemotaxis of *Agrobacterium tumefaciens* C58C[1] toward *vir*-inducing phenolic compounds and soluble factors from monocotyledonous and dicotyledonous plants. J. Bacteriol. **170:**4181–4187.
7. **Merritt PM, Danhorn T, Fuqua C.** 2007. Motility and chemotaxis in

Agrobacterium tumefaciens surface attachment and biofilm formation. J. Bacteriol. **189:**8005–8014. http://dx.doi.org/10.1128/JB.00566-07.

8. **Abarca-Grau AM, Penyalver R, Lopez MM, Marco-Noales E.** 2011. Pathogenic and non-pathogenic *Agrobacterium tumefaciens*, *A. rhizogenes* and *A. vitis* strains form biofilms on abiotic as well as on root surfaces. Plant Pathol. **60:**416–425. http://dx.doi.org/10.1111/j.1365-3059.2010.02385.x.
9. **Matthysse AG.** 1983. Role of bacterial cellulose fibrils in *Agrobacterium tumefaciens* infection. J. Bacteriol. **154:**906–915.
10. **Breedveld MW, Miller KJ.** 1994. Cyclic beta-glucans of members of the family *Rhizobiaceae*. Microbiol. Rev. **58:**145–161.
11. **Gelvin SB.** 2003. *Agrobacterium*-mediated plant transformation: the biology behind the "gene-jockeying" tool. Microbiol. Mol. Biol. Rev. **67:**16–37. http://dx.doi.org/10.1128/MMBR.67.1.16-37.2003.
12. **Xu J, Kim J, Koestler BJ, Choi JH, Waters CM, Fuqua C.** 2013. Genetic analysis of *Agrobacterium tumefaciens* unipolar polysaccharide production reveals complex integrated control of the motile-to-sessile switch. Mol. Microbiol. **89:**929–948. http://dx.doi.org/10.1111/mmi.12321.
13. **Lassalle F, Campillo T, Vial L, Baude J, Costechareyre D, Chapulliot D, Sham M, Abrouk D, Lavire C, Oger-Desfeux C, Hommais F, Guequen L, Daubin V, Muller D, Nesme X.** 2011. Genomic species are ecological species as revealed by comparative genomics in *Agrobacterium tumefaciens*. Genome Biol. Evol. **3:**762–781. http://dx.doi.org/10.1093/gbe/evr070.
14. **Kachlany SC, Planet PJ, Desalle R, Fine DH, Figurski DH, Kaplan JB.** 2001. *flp-1*, the first representative of a new pilin gene subfamily, is required for non-specific adherence of *Actinobacillus actinomycetemcomitans*. Mol. Microbiol. **40:**542–554. http://dx.doi.org/10.1046/j.1365-2958.2001.02422.x.
15. **Bodenmiller D, Toh E, Brun Y.** 2004. Development of surface adhesion in *Caulobacter crescentus*. J. Bacteriol. **186:**1438–1447. http://dx.doi.org/10.1128/JB.186.5.1438-1447.2004.
16. **Chen L, Chen Y, Wood DW, Nester EW.** 2002. A new type IV secretion system promotes conjugal transfer in *Agrobacterium tumefaciens*. J. Bacteriol. **184:**4838–4845. http://dx.doi.org/10.1128/JB.184.17.4838-4845.2002.
17. **von Bodman SB, McCutchan JE, Farrand SK.** 1989. Characterization of conjugal transfer functions of *Agrobacterium tumefaciens* Ti plasmid pTiC58. J. Bacteriol. **171:**5281–5289.
18. **Fullner KJ, Lara JC, Nester EW.** 1996. Pilus assembly by Agrobacterium T-DNA transfer genes. Science **273:**1107–1109. http://dx.doi.org/10.1126/science.273.5278.1107.
19. **Cook DM, Li PL, Ruchaud F, Padden S, Farrand SK.** 1997. Ti plasmid conjugation is independent of vir: reconstitution of the tra functions from pTiC58 as a binary system. J. Bacteriol. **179:**1291–1297.
20. **Lai EM, Chesnokova O, Banta LM, Kado CI.** 2000. Genetic and environmental factors affecting T-pilin export and T-pilus biogenesis in relation to flagellation of *Agrobacterium tumefaciens*. J. Bacteriol. **182:**3705–3716. http://dx.doi.org/10.1128/JB.182.13.3705-3716.2000.
21. **Wood DW, Setubal JC, Kaul R, Monks DE, Kitajima JP, Okura VK, Zhou Y, Chen L, Wood GE, Almeida NF, Jr, Woo L, Chen Y, Paulsen IT, Eisen JA, Karp PD, Bovee Sr D, Chapman P, Clendenning J, Deatherag G, Gillet W, Grant C, Kutyavin T, Levy R, Li MJ, McClelland E, Palmieri P, Raymond C, Rouse R, Saenphimmachak C, Wu Z, Romero P, Gordon D, Zhang S, Yoo H, Kim S, Hendrick C, Zhao ZY, Dolan M, Chumley F, Tingey SV, Tomb JF, Gordon MP, Olsen MV, Nester EW.** 2001. The genome of the natural genetic engineer *Agrobacterium tumefaciens* C58. Science **294:**2317–2323. http://dx.doi.org/10.1126/science.1066804.
22. **Goodner B, Hinkle G, Gattung S, Miller N, Blanchard M, Qurollo B, Goldman SB, Cao YW, Askenazi M, Iartchouk O, Epp A, Liu F, Wollam C, Allinger M, Doughty D, Scott C, Lappas C, Markelz B, Flanagan C, Crowell C, Gurson J, Lomo C, Sear C, Strub G, Cielo C, Slatte S.** 2001. Genome sequence of the plant pathogen and biotechnology agent *Agrobacterium tumefaciens* C58. Science **294:**2323–2328. http://dx.doi.org/10.1126/science.1066803.
23. **Skerker JM, Shapiro L.** 2000. Identification and cell cycle control of a novel pilus system in *Caulobacter crescentus*. EMBO J. **19:**3223–3234. http://dx.doi.org/10.1093/emboj/19.13.3223.
24. **Tomich M, Planet PJ, Figurski DH.** 2007. The *tad* locus: postcards from the widespread colonization island. Nat. Rev. Microbiol. **5:**363–375. http://dx.doi.org/10.1038/nrmicro1636.
25. **Inoue T, Tanimoto I, Ohta H, Kato K, Murayama Y, Fukui K.** 1998. Molecular characterization of low-molecular-weight component protein, Flp, in *Actinobacillus actinomycetemcomitans* fimbriae. Microbiol. Immunol. **42:**253–258. http://dx.doi.org/10.1111/j.1348-0421.1998.tb02280.x.
26. **Rosenfeld JA, Sarkar IN, Planet PJ, Figurski DH, DeSalle R.** 2004. ORFcurator: molecular curation of genes and gene clusters in prokaryotic organisms. Bioinformatics **20:**3462–3465. http://dx.doi.org/10.1093/bioinformatics/bth427.
27. **Inoue T, Ohta H, Kokeguchi S, Fukui K, Kato K.** 1990. Colonial variation and fimbriation of *Actinobacillus actinomycetemcomitans*. FEMS Microbiol. Lett. **69:**13–18. http://dx.doi.org/10.1111/j.1574-6968.1990.tb04167.x.
28. **Sambrook J, Fritsch EF, Maniatis T.** 1989. Molecular cloning: a laboratory manual, 2nd ed. Cold Spring Harbor Laboratory Press, Cold Spring Harbor, NY.
29. **Mersereau M, Pazour GJ, Das A.** 1990. Efficient transformation of *Agrobacterium tumefaciens* by electroporation. Gene **90:**149–151. http://dx.doi.org/10.1016/0378-1119(90)90452-W.
30. **Tempé J, Petit A, Holsters M, Montagu MV, Schell J.** 1977. Thermosensitive step associated with transfer of Ti plasmid during conjugation—possible relation to transformation in crown gall. Proc. Natl. Acad. Sci. U. S. A. **74:**2848–2849. http://dx.doi.org/10.1073/pnas.74.7.2848.
31. **Warrens AN, Jones MD, Lechler RI.** 1997. Splicing by overlap extension by PCR using asymmetric amplification: an improved technique for the generation of hybrid proteins of immunological interest. Gene **186:**29–35. http://dx.doi.org/10.1016/S0378-1119(96)00674-9.
32. **Khan SR, Gaines J, Roop RM, Farrand SK.** 2008. Broad-host-range expression vectors with tightly regulated promoters and their use to examine the influence of TraR and TraM expression on Ti plasmid quorum sensing. Appl. Environ. Microbiol. **74:**5053–5062. http://dx.doi.org/10.1128/AEM.01098-08.
33. **Miller JH.** 1972. Experiments in molecular genetics. Cold Spring Harbor Laboratory, Cold Spring Harbor, NY.
34. **Morton ER, Fuqua C.** 2012. Phenotypic analyses of *Agrobacterium*. Curr. Protoc. Microbiol. **Chapter 3:**Unit 3D.3. http://dx.doi.org/10.1002/9780471729259.mc03d03s25.
35. **Anand VK, Heberlein GT.** 1977. Crown gall tumorigenesis in potato tuber tissue. Am. J. Bot. **64:**153–158. http://dx.doi.org/10.2307/2442102.
36. **Heydorn A, Nielsen AT, Hentzer M, Sternberg C, Givskov M, Ersball BK, Molin S.** 2000. Quantification of biofilm structures by the novel computer program COMSTAT. Microbiology **146**(Pt 10)**:**2395–2407.
37. **Kachlany SC, Planet PJ, Bhattacharjee MK, Kollia E, DeSalle R, Fine DH, Figurski DH.** 2000. Nonspecific adherence by *Actinobacillus actinomycetemcomitans* requires genes widespread in *Bacteria* and *Archaea*. J. Bacteriol. **182:**6169–6176. http://dx.doi.org/10.1128/JB.182.21.6169-6176.2000.
38. **de Bentzmann S, Aurouze M, Ball G, Filloux A.** 2006. FppA, a novel *Pseudomonas aeruginosa* prepilin peptidase involved in assembly of type IVb pili. J. Bacteriol. **188:**4851–4860. http://dx.doi.org/10.1128/JB.00345-06.
39. **Perez BA, Kachlany SC, Tomich M, Fine DH, Figurski DH.** 2006. Genetic analysis of the requirement for *flp-2*, *tadV*, and *rcpB* in *Actinobacillus actinomycetemcomitans* biofilm formation. J. Bacteriol. **188:**6361–6375. http://dx.doi.org/10.1128/JB.00496-06.
40. **Morton ER, Platt TG, Fuqua C, Bever JD.** 2014. Non-additive costs and interactions alter the competitive dynamics of co-occurring ecologically distinct plasmids. Proc. Biol. Sci. **281:**20132173. http://dx.doi.org/10.1098/rspb.2013.2173.
41. **Xu J, Kim J, Danhorn T, Merritt PM, Fuqua C.** 2012. Phosphorus limitation increases attachment in *Agrobacterium tumefaciens* and reveals a conditional functional redundancy in adhesin biosynthesis. Res. Microbiol. **163:**674–684. http://dx.doi.org/10.1016/j.resmic.2012.10.013.
42. **Li G, Brown PJ, Tang JX, Xu J, Quardokus EM, Fuqua C, Brun YV.** 2012. Surface contact stimulates the just-in-time deployment of bacterial adhesins. Mol. Microbiol. **83:**41–51. http://dx.doi.org/10.1111/j.1365-2958.2011.07909.x.
43. **Tomich M, Fine DH, Figurski DH.** 2006. The TadV protein of *Actinobacillus actinomycetemcomitans* is a novel aspartic acid prepilin peptidase required for maturation of the Flp1 pilin and TadE and TadF pseudopilins. J. Bacteriol. **188:**6899–6914. http://dx.doi.org/10.1128/JB.00690-06.
44. **Bhattacharjee MK, Kachlany SC, Fine DH, Figurski DH.** 2001. Nonspecific adherence and fibril biogenesis by *Actinobacillus actinomycetemcomitans*: TadA protein is an ATPase. J. Bacteriol. **183:**5927–5936. http://dx.doi.org/10.1128/JB.183.20.5927-5936.2001.